

Supporting Information

Bright green electroluminescence with an EQE of 4.6% from a host-guest OLED fabricated from an unsymmetric liquid crystalline N-annulated perylene ester imide as a dopant

Paresh Kumar Behera,^a Feng-Rong Chen,^b Jwo-Huei Jou*^b and
Ammathnadu Sudhakar Achalkumar*^{a,c}

*^aDepartment of Chemistry, Indian Institute of Technology Guwahati,
Guwahati, 781039, Assam, India.*

*^bDepartment of Materials Science and Engineering National Tsing Hua University 101, Sec.
2, Kuang-Fu Road, Hsinchu 30013, Taiwan*

*^cCentre for Sustainable Polymers, Indian Institute of Technology Guwahati,
Guwahati, 781039, Assam, India.*

Table of Contents

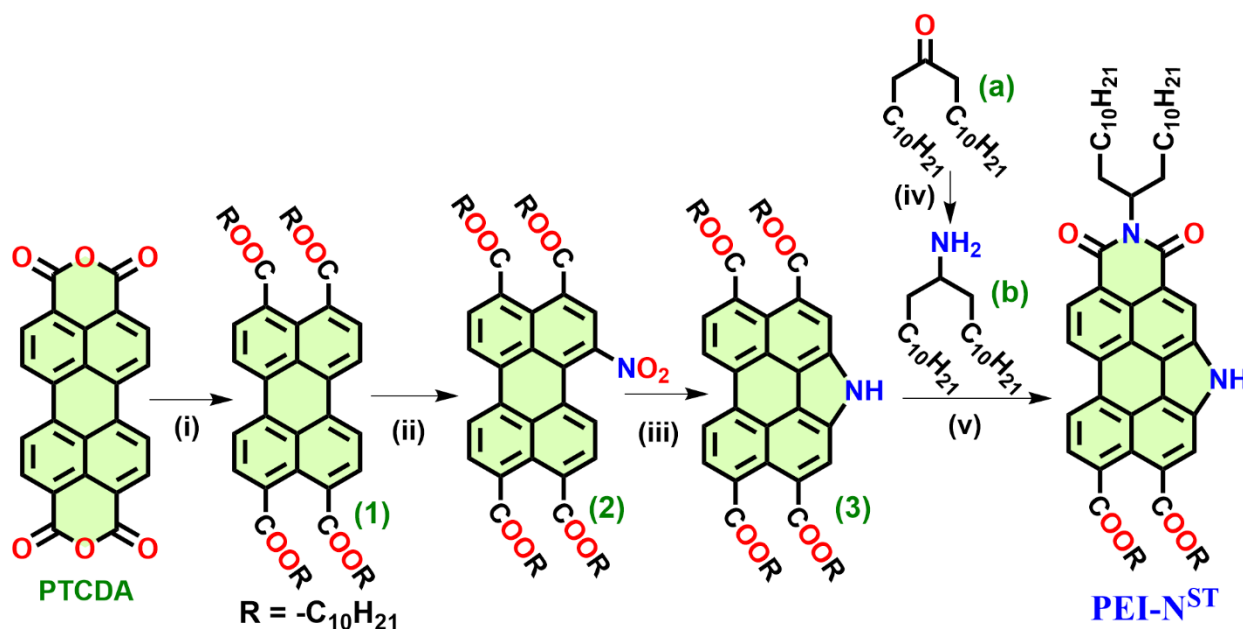
Serial Number	Contents	Page numbers
1	Materials and methods	S3
2	Experimental Section	S4-S5
3	NMR Spectra	S6
4	MALDI-TOF mass spectrometry	S7
5	Photophysical studies	S7-S8
6	Quantum yield measurement	S8-S9
7	Polarizing Optical Microscopy (POM)	S9
8	Differential Scanning Calorimetry (DSC)	S10
9	Thermogravimetric analysis (TGA)	S10
10	X-ray diffraction (XRD) studies	S11
11	Cyclic Voltammetry	S12
12	Device Fabrication and characterization	S12-S15
13	DFT Studies	S15-S17
14	Time resolved photoluminescence studies	S17
15	References	S18

1. Materials and methods

Commercially available chemicals were utilized without further purification, and standard procedures were followed to dry the solvents. Chromatography was conducted using either silica gel (60-120 mesh) or neutral aluminum oxide. For thin-layer chromatography, aluminum sheets pre-coated with silica gel were employed. IR spectra were acquired at room temperature using a Perkin Elmer IR spectrometer (PerkinElmer UATR TWO). The spectral positions are reported in wave number (cm^{-1}) units. NMR spectra were recorded using a 600MHz Nuclear Magnetic Resonance (NMR) Spectrometer (Make: Bruker, Model: AVANCE III HD). Chemical shifts in ^1H NMR spectra were referenced to TMS as an internal standard and reported in ppm. Coupling constants were provided in Hz. Mass spectra were obtained using a MALDI-TOF mass spectrometer (Matrix Assisted Laser Desorption Ionization- Time of Flight, Make: BRUKER Model: AUTOFLEX SPEED) with α -Cyano-4-hydroxycinnamic acid as a matrix. The liquid crystalline behavior of the mesogenic compounds, including birefringence and fluidity, was investigated using a polarizing optical microscope (Nikon Eclipse LV100POL) equipped with a programmable hot stage (Mettler Toledo FP90). Observations were made with clean glass slides and coverslips. Differential scanning calorimetry (DSC) under a nitrogen atmosphere was used to determine transition temperatures and associated enthalpy changes. A Mettler Toledo DSC1 instrument was employed, and the peak temperatures corresponding to transitions obtained from DSC were consistent with the polarizing optical microscopic observations. The first heating and cooling cycles were conducted at a rate of $5\text{ }^\circ\text{C}/\text{min}$, and the transition temperatures were recorded. Variable temperature XRD studies were performed using samples filled in Lindemann capillaries. A high-resolution X-ray powder diffractometer (PANalytical X'Pert PRO) equipped with a high-resolution fast detector PIXCEL was used. The sample temperature was controlled using a Mettler hot stage/programmer (FP82HT/FP90). Thermogravimetric analysis (TGA) was carried out using a thermogravimetric analyzer (Mettler Toledo, model TG/SDTA 851 e) under a nitrogen flow at a heating rate of $10\text{ }^\circ\text{C}/\text{min}$. UV-Vis spectra were recorded using a Perkin-Elmer Lambda 750 UV/VIS/NIR spectrometer. Fluorescence emission in solution state was investigated using either a Horiba Fluoromax-4 fluorescence spectrophotometer or a Perkin Elmer LS 50B spectrometer. Cyclic Voltammetry (CV) studies were conducted using a Metrohm Autolab PGSTAT204 Electrochemical workstation with the assistance of NOVA software.

2. Experimental Section:

2.1. Synthetic Scheme



Reagents and conditions: (i) KOH, H₂O, 70 °C, 0.5 h, 1 M HCl, Aliquat 336, KI, 1-bromobutane, reflux, 12 h (76%); (ii) NaNO₂, HNO₃, 0 °C, 1 h (90%); (iii) triethyl phosphite, 160 °C, reflux, 4 h, N₂ atmosphere (60%); (iv) NH₄OAc, NaBH₃CN, MeOH, RT, 72 h (95%); (v) b, Zn(OAc)₂, imidazole, 150 °C, 25 min, 30W, 100 psi, MW (47%).

Compounds 1, ^[S1] 2, 3, ^[S1] were prepared as reported earlier.

2.2 Synthetic Procedure

2.2.1 Synthetic route of Tricosan-12-amine (b):

A 250 mL round-bottom flask was charged with 12-tricosanone (a) (5 g, 14.76 mmol), NH₄OAc (11.35 g, 147.6 mmol), NaBH₃CN (1.275 g, 1.38 mmol) and MeOH (100 mL) and stirred at room temperature (r.t.) for 72 h, until the starting material was consumed (monitored by TLC). The reaction was quenched by drop wise addition of conc. HCl (~12 mL) and the solvents removed by rotary evaporation. The resulting white solid was dissolved in H₂O (200 mL) and adjusted to pH ~10 with KOH, then extracted with CHCl₃ (3 × 150 mL) to give the desired product as a white solid (4.8g, 95.6%). ¹H-NMR (600MHz, CDCl₃): δ = 0.88 (t, 6H), 1.10-1.50 (m, 42H), 2.68 ppm (s, 1H).

2.2.2 General procedure for synthesis of PEI-NST:

Compound **3** (1 eq.), tricosan-12-amine (1.1 eq.), zinc acetate (1 eq.) and imidazole (1 g) were taken in a microwave vessel, flushed with nitrogen and placed in a microwave reactor. The mixture was heated to 150 °C for 30 minutes at 35 W and 100 psi pressure. After cooling, the reaction mixture was poured into a 2N HCl (10 mL) solution and extracted with chloroform. Organic layer was washed with water and saturated sodium chloride solution. The crude compound was purified by column chromatography on neutral alumina using 5% chloroform-hexane system. Further purification was done by repeated recrystallization from THF-methanol system.

PEI-NST: $R_f = 0.5$ (10% CHCl₃-Hexane); Bright red powdered solid, yield: 47 %; IR ν_{\max} in cm⁻¹: 3299, 2919, 2851, 1708, 1684, 1650, 1600, 1464, 1413, 1321, 1254, 1196, 1153, 1088, 1047, 835, 747, 722; ¹H NMR (600 MHz, CDCl₃, ppm): δ 9.76 (s, 1H, NH_{Ar}), 8.56 (d, $J = 6$ Hz, 1H, H_{Ar}), 8.52 (d, $J = 12$ Hz, 1H, H_{Ar}), 8.39 (d, $J = 6$ Hz, 1H, H_{Ar}), 8.31 (s, 1H, H_{Ar}), 8.25 (s, 1H, H_{Ar}), 8.23 (d, $J = 6$ Hz, 1H, H_{Ar}), 5.37 (m, 1H, NCH), 4.52 (t, $J = 7.2$ Hz, 2H, -OCH₂), 4.48 (t, $J = 6$ Hz, 2H, -OCH₂), 2.39 (m, 2H), 1.99 (m, 2H), 1.95-1.89 (m, 4H), 1.56-1.51 (m, 4H), 1.47-1.17 (m, 60H), 0.86 (t, $J = 6$ Hz, 6H, 2 × CH₃), 0.80 (t, $J = 7.2$ Hz, 6H, 2 × CH₃). ¹³C NMR (150 MHz, CDCl₃) δ 169.49, 169.42, 166.46, 165.40, 165.21, 164.23, 132.56, 132.45, 132.19, 131.25, 130.75, 129.88, 129.62, 127.95, 127.52, 127.19, 123.93, 123.76, 123.55, 122.55, 121.45, 121.03, 120.65, 120.23, 120.06, 119.87, 119.66, 119.48, 119.25, 117.30, 77.23, 77.02, 76.81, 66.31, 66.17, 54.59, 54.51, 32.74, 32.64, 31.94, 31.92, 31.87, 29.74, 29.66, 29.61, 29.50, 29.48, 29.39, 29.36, 29.31, 28.81, 27.31, 27.27, 26.19, 26.16, 22.71, 22.69, 22.63, 14.11, 14.06. MALDI-TOF exact mass calculated for C₆₇H₉₇N₂O₆(M+H)⁺: 1025.735, found: 1025.420.

3. NMR Spectra

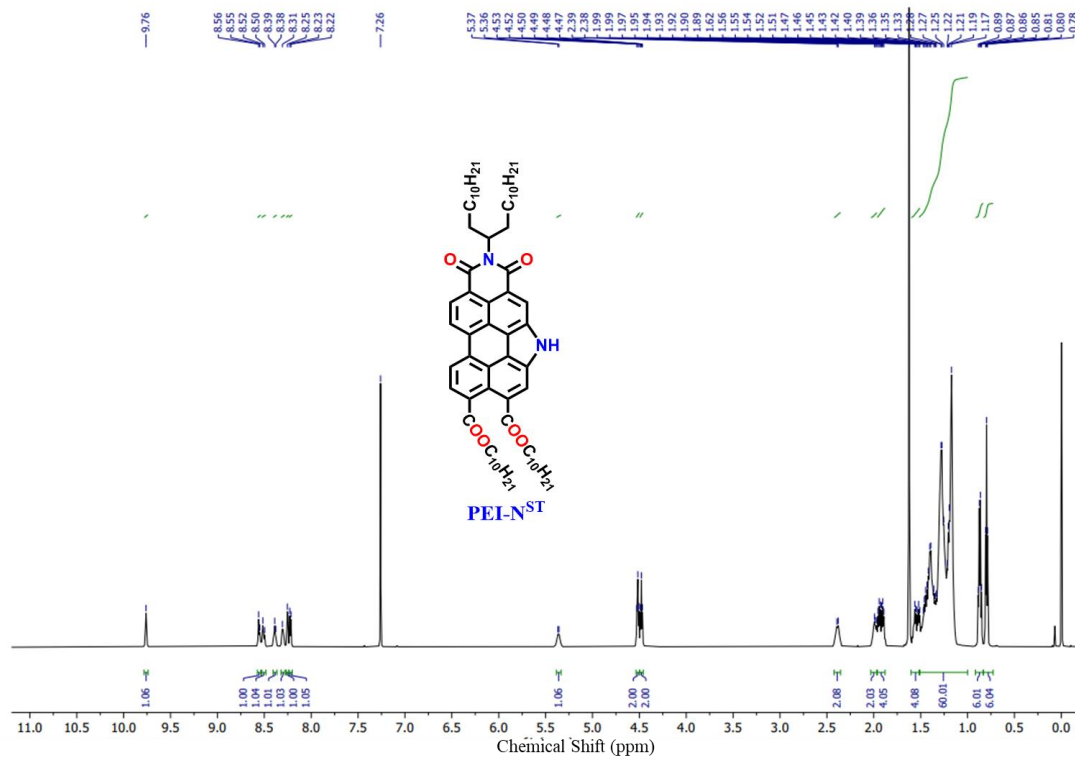


Figure S1. ^1H NMR (600 MHz) spectra of PEI-NST in CDCl_3 .

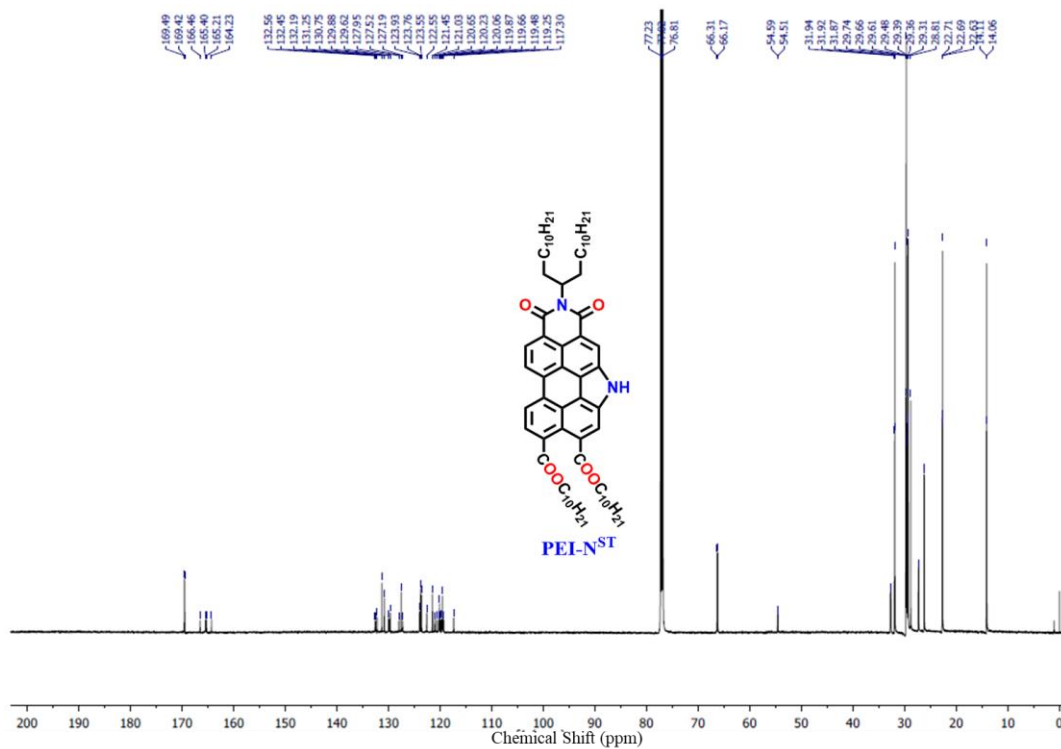


Figure S2. ^{13}C NMR (150 MHz) spectra of PEI-NST in CDCl_3 .

4. MALDI-TOF mass spectrometry

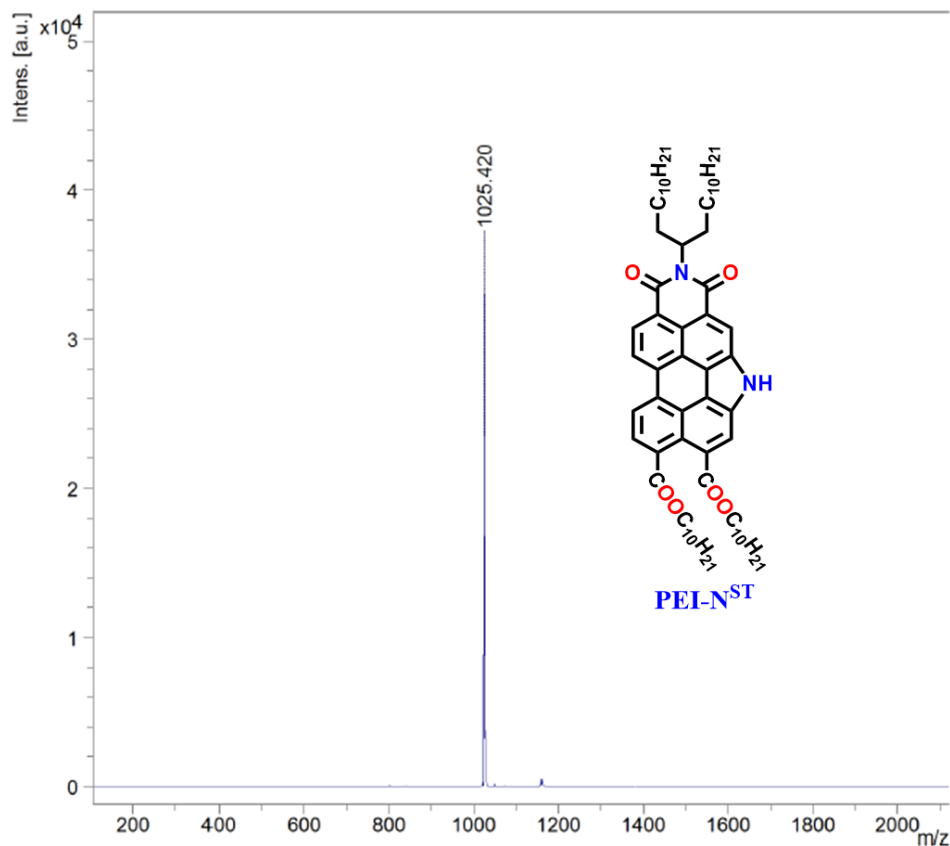


Figure S3. MALDI-TOF mass spectrum of PEI-NST.

5. Photophysical studies

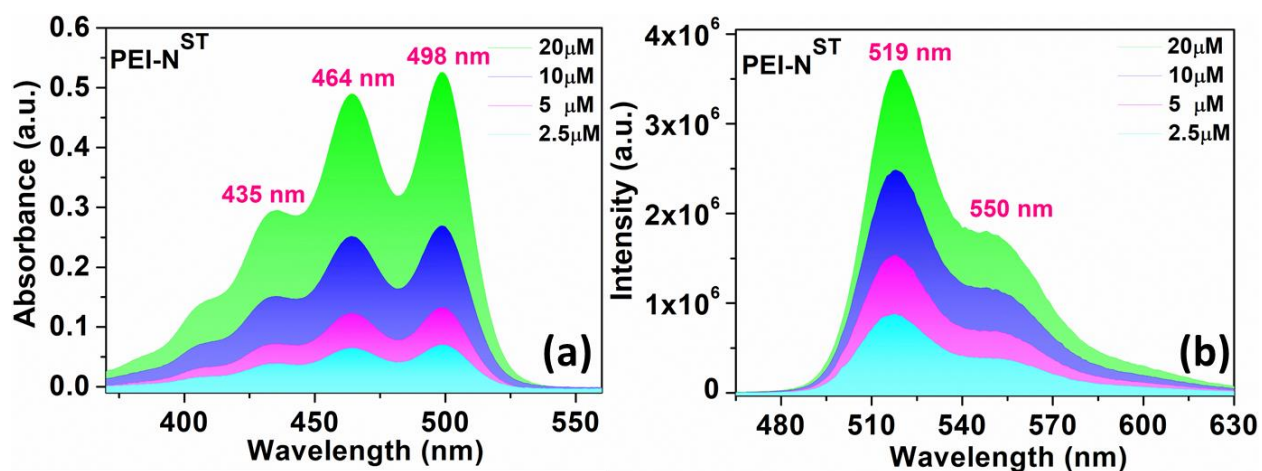


Figure S4. Absorption (a) emission (b) spectra of PEI-NST in chloroform solution as a function of concentration.

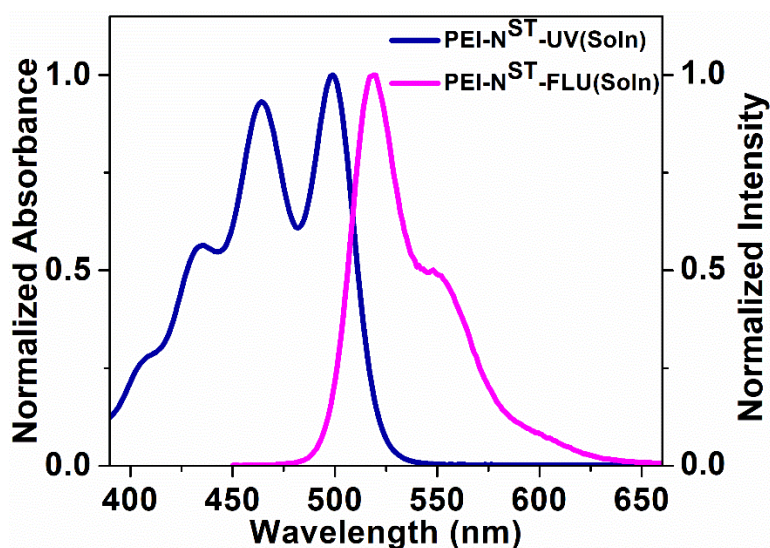


Figure S5. Overlay of absorption and emission spectra of **PEI-NST** in chloroform solution.

Table S1. Photophysical properties of **PEI-NST** in solution^a and thin film^b state.

Entry	Absorption [nm]	Emission ^c [nm]	Stokes Shift (cm ⁻¹)	Molar extinction coefficient (ε) (L mol ⁻¹ cm ⁻¹)	Quantum yield ^d (Q _S)	ΔE _{g, opt} ^e [eV]	Absorption [nm]	Emission ^f [nm]	Stokes Shift (cm ⁻¹)
PEI-NST	406, 435, 464, 498	519, 550	813	26,866	0.91	2.37	464, 521	616	5158

^aMicromolar solutions in CHCl₃. ^bPrepared by drop casting of millimolar solution in toluene. ^cThe excitation wavelength λ_{ex} = 498 nm **PEI-NST**. ^dRelative quantum yields are calculated with respect to Rhodamine-6G (λ_{ex} = 530 nm) in ethanol solution as the standard and compounds in CHCl₃. ^eCalculated from the red edge of the absorption band. ^fExcited at the absorption maxima.

6. Quantum yield measurement (Relative)

Quantum yield was measured according to established procedure by using rhodamine 6g in ethanol as the standard. Absolute values were calculated according to the following equation:

$$Q_S = Q_R \times (m_S / m_R) \times (n_S / n_R)^2,$$

Where, Q: Quantum yield, m: Slope of the plot of integrated fluorescence intensity vs absorbance (Calculated from Fig.S15), n: refractive index (1.361 for ethanol and 1.445 for chloroform). The subscript R refers to the reference fluorophore i.e. rhodamine 6G solution in EtOH and subscript S refers to the sample under investigation. In order to minimize re-absorption effects, absorbance was kept below 0.15 at the excitation wavelength of 498 nm for compound **PEI-NST**. Quantum yield of rhodamine 6g in EtOH is 0.95. Simplified equation for the calculation after substituting the appropriate values is given below and values obtained are given in table below.

$$Q_S = 0.95 \times (m_S / m_R) \times (1.445/1.361)^2$$

Compounds	ms	mr	Q _s ^{a,b,c}
PEI-N ST	5.65079×10^8	6.53162×10^8	0.91

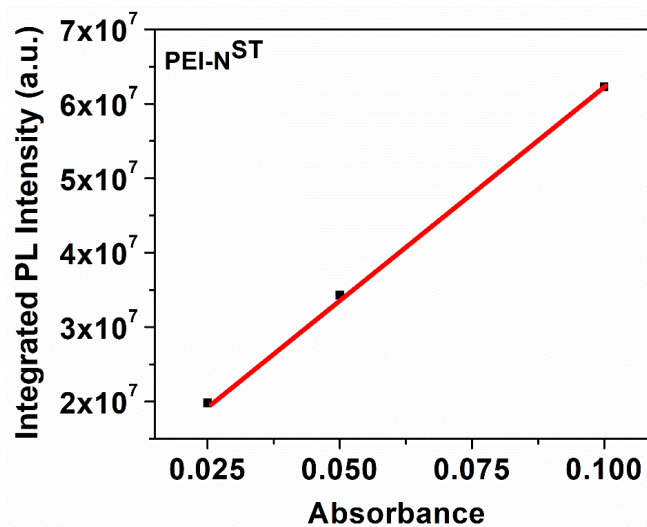


Figure S6. Plot of integrated photoluminescence intensity vs absorbance of compound PEI-NST.

7. Polarizing Optical Microscopy (POM)

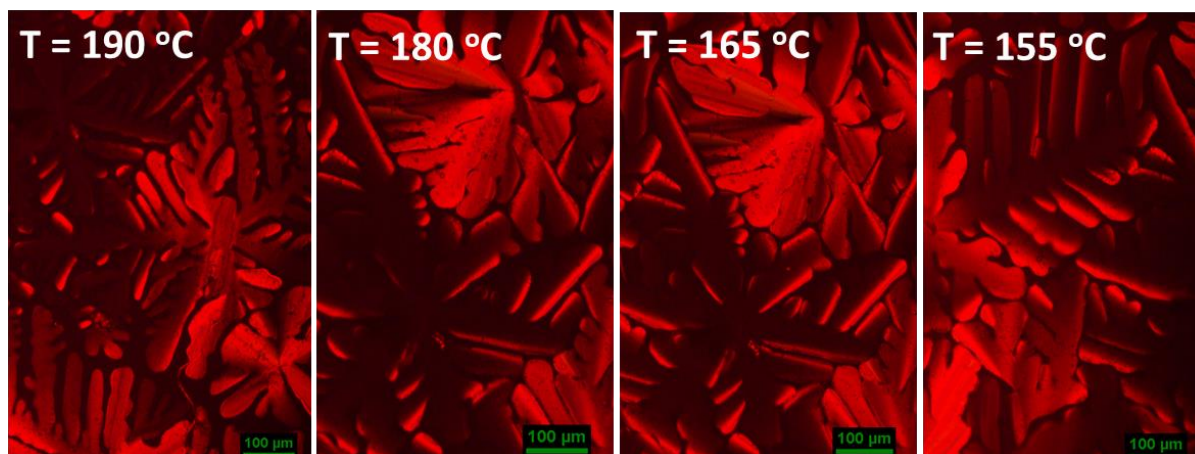


Figure S7. POM images obtained PEI-NST at different temperatures (scale bar 100 μm).

8. Differential Scanning Calorimetry (DSC)

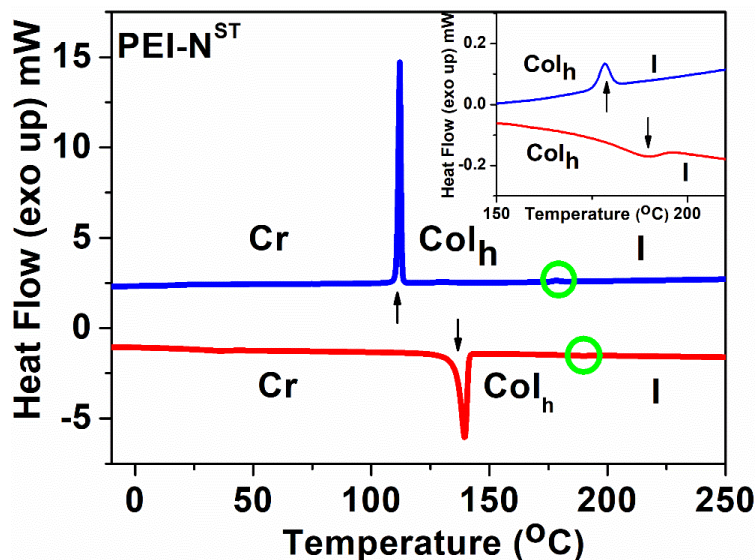


Figure S8. DSC thermograms of PEI-N^{ST} carried out at a rate of $5^\circ\text{C}/\text{min}$ (red trace: second heating, blue trace: first cooling).

Table S2. Phase transition temperatures ($^\circ\text{C}$), corresponding enthalpies (kJmol^{-1})^a and decomposition temperatures^b of PEI-N^{ST} obtained from DSC^a and TGA^b.

Entry	Phase Sequence (kJ/mol)		T_5^b ($^\circ\text{C}$)
	Second heating	First Cooling	
PEI-N^{ST}	Cr 138.32 (34.2) Col _h 190.4 (0.18) I	I 179.5 (0.22) Col _h 113.1 (36.9) Cr	367

^a Peak temperatures in the DSC thermograms obtained during the second heating and first cooling cycles at 5°C min^{-1} Col_h = Columnar hexagonal phase; I = Isotropic phase; ^bTemperature at which 5 weight % decomposition occurs as noted from TGA;

9. Thermogravimetric analysis (TGA)

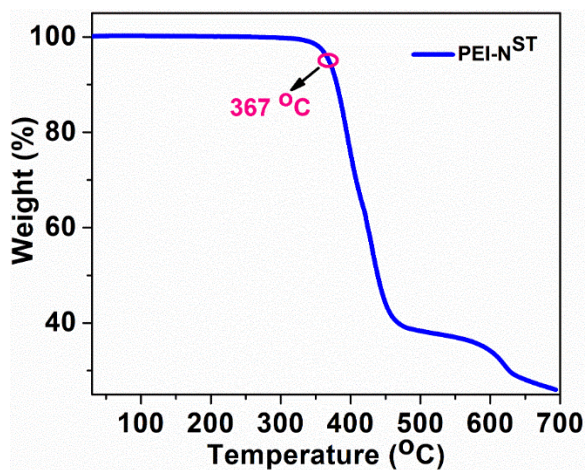


Figure S9. TGA plots of compound PEI-N^{ST} (heating rate of $10^\circ\text{C}/\text{min}$, Nitrogen atmosphere).

10. X-ray diffraction studies (XRD)

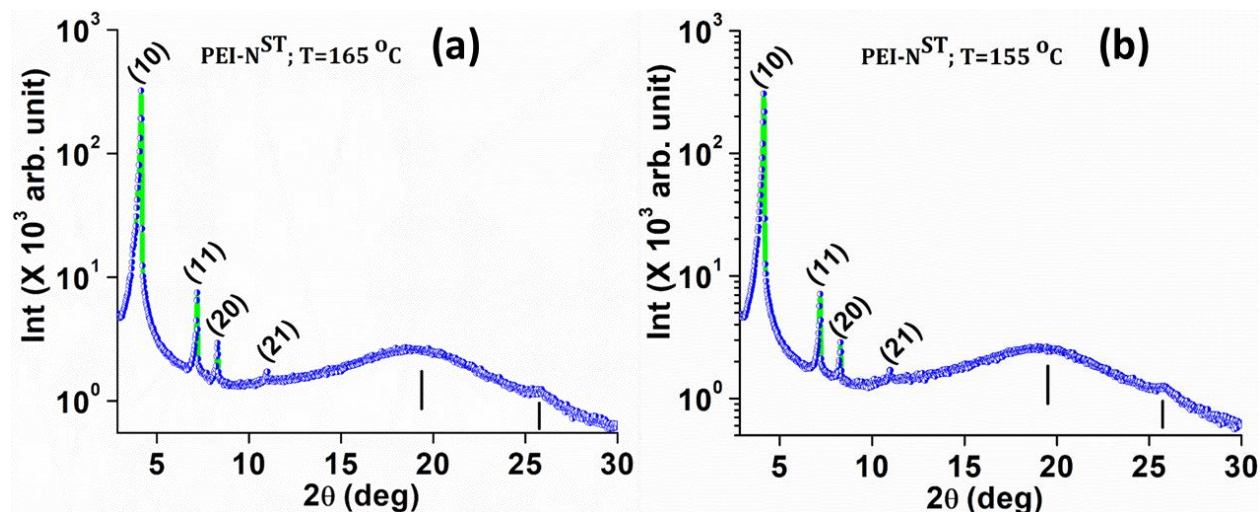


Figure S10. Plot of the intensity against 2θ obtained from the powder XRD pattern of the Col_h phases PEI-N^{ST} at different temperature intervals.

Table S3. Results of (hkl) indexation of XRD profiles of the compounds at a given temperature (T) of mesophases.^a

Compounds (D/Å)	Phase (T/°C)	d_{obs} (Å)	d_{cal} (Å)	Miller indices hkl	Lattice parameters (Å), Lattice area S (Å ²), Molecular volume (Å ³)
PEI-N^{ST} (34 Å) MW: 1025.4	Col_h (165)	21.28	21.28	100	$a = 24.6$ $S = 522.3$ $V = 1796.1$ $Z \approx 1$
		12.27	12.28	110	
		10.64	10.64	200	
		8.04	8.04	210	
		4.73 (h_a)			
		3.44 (h_c)			
	Col_h (155)	20.29	20.29	100	$a = 23.4$ $S = 475.4$ $V = 1640$ $Z \approx 1$
		12.27	11.71	110	
		10.65	10.14	200	
		8.05	7.66	210	
		4.68 (h_a)			
		3.45 (h_c)			

^aThe diameter (D) of the disk (estimated from Chem 3D Pro 8.0 molecular model software from Cambridge Soft). d_{obs} : spacing observed; d_{cal} : spacing calculated (deduced from the lattice parameters; a for Col_h phase; c is height of the unit cell). The spacings marked h_a and h_c correspond to diffuse reflections in the wide-angle region arising from correlations between the alkyl chains and core regions, respectively.

11. Cyclic Voltammetry

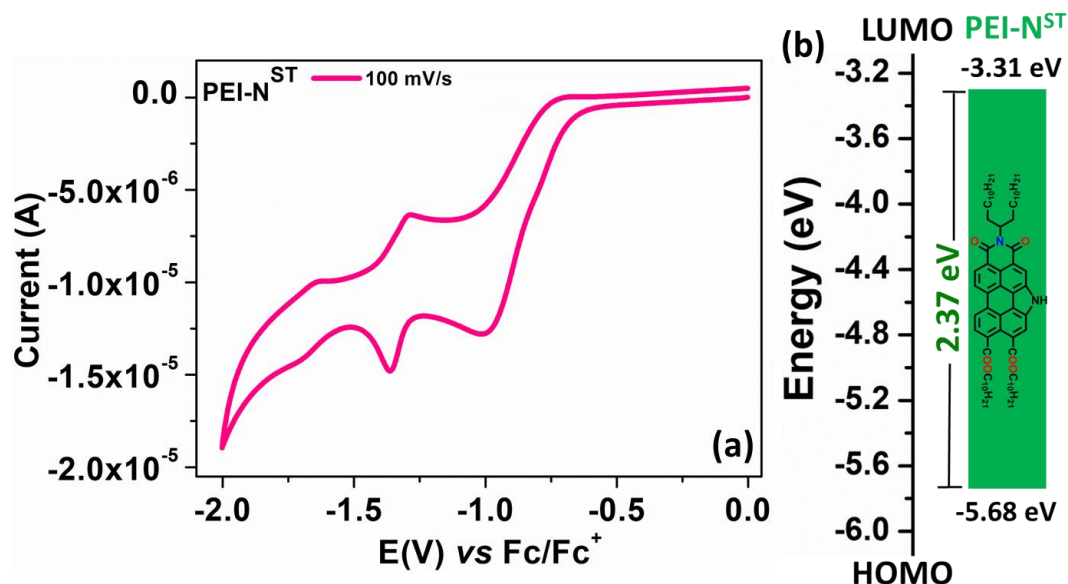


Figure S11. Cyclic voltammograms of **PEI-NST**(a); Energy band level diagram showing HOMO and LUMO energy levels.

Table S4. Electrochemical^{a,b} data and data obtained from DFT^h calculations for **PEI-NST**

Electrochemical data					Data from DFT calculations		
Entry	$E_{1st\ red}^{[c]}$	$E_{LUMO}^{[d,e]}$	$E_{HOMO}^{[d,f]}$	$\Delta E_{g,opt}^{[d,g]}$	$E_{LUMO}^{[d,h]}$	$E_{HOMO}^{[d,h]}$	$\Delta E_g^{[d,h]}$
PEI-NST	-0.99	-3.31	-5.68	2.37	-2.85	-5.65	2.80

[^a] 0.5 mM Dichloromethane solutions; [^b] experimental conditions: Ag/AgNO₃ as reference electrode, glassy carbon working electrode, platinum wire counter electrode, TBAP (0.1M) as a supporting electrolyte, room temperature; [^c] in volts (V); [^d] in eV; [^e] estimated from the formula by using $E_{LUMO} = -(4.8 - E_{1/2, Fc/Fc^+} + E_{red, onset})$ eV; [^f] estimated from the formula $E_{HOMO} = (E_{LUMO} - E_{g,opt})$ eV; $E_{1/2, Fc/Fc^+} = 0.50$ V. [^g] calculated from the red edge of the absorption band of each compound. [^h] Obtained from DFT calculations by employing the combination of Becke3-Lee-Yang-Parr (B3LYP) hybrid functional and 6-31G(d,p) basis set using the Gaussian 09 package.

12. Device fabrication and characterization

Based on superior photophysical and electrochemical properties, the electroluminescent properties of **PEI-NST** emitter material, was investigated. Multi-layered solution processed OLED was fabricated consisting of following device configurations: anode: ITO (125 nm)/HIL: PEDOT:PSS (40 nm)/ EML (20 nm)/ ETL: TPBi (35 nm)/EIL: LiF (1 nm)/cathode: Al (100 nm). Initially, ITO-coated glass substrates were cleaned to remove greasy layer. The cleaning process was carried-out with soap-solution, deionized water, acetone, and alcohol in water-bath sonicator at optimized time. Cleaned substrates were kept in ultra-violet ozone system to expose in UV-light

for removing residual solvents and further impurities. Then, these substrates were transferred into nitrogen purged glovebox for further processing of layers. Simultaneously, CBP as host and newly synthesized emitter (**PEI-NST**) for emissive solution layer was dispersed into suitable solvents with water-bath sonicator. Prepared solution was filtered with 0.45 μm PTFE filters and mixed in desired ratio to prepare emissive layer. First, a hole-injection layer was prepared by spin-coating an aqueous solution of PEDOT:PSS at 4,000 rpm for 20 s. Subsequently, these substrates were annealed at 130 $^{\circ}\text{C}$ for 15 minutes. After cooled down the substrates, neat solution or emissive layer solution was spin-coated onto hole-injection layer at 2,500 rpm for 20 s. Then, these substrates were transferred into thermal evaporator to deposit subsequent layers. Then, TPBi was deposited as an electron-transport layer followed by the deposition of 0.5 nm LiF as an electron-injection layer and 100 nm Al as a cathode. All the layers of TPBi, LiF and Al were deposited subsequently via thermal evaporation method at base pressure of 4.0×10^{-6} Torr. After that, Fabricated devices were kept in the mini vacuum chamber during testing process and then measured at room temperature conditions. To analyse the device, the electroluminescence (EL) spectrum, luminance, and the CIE coordinates were obtained using a photo research (PR-655) spectrometer. The current density-voltage-luminance (J-V-L) characteristics were obtained by a computer mounted voltmeter (Keithley 2400) and spectrophotometer CS-100 Minolta.

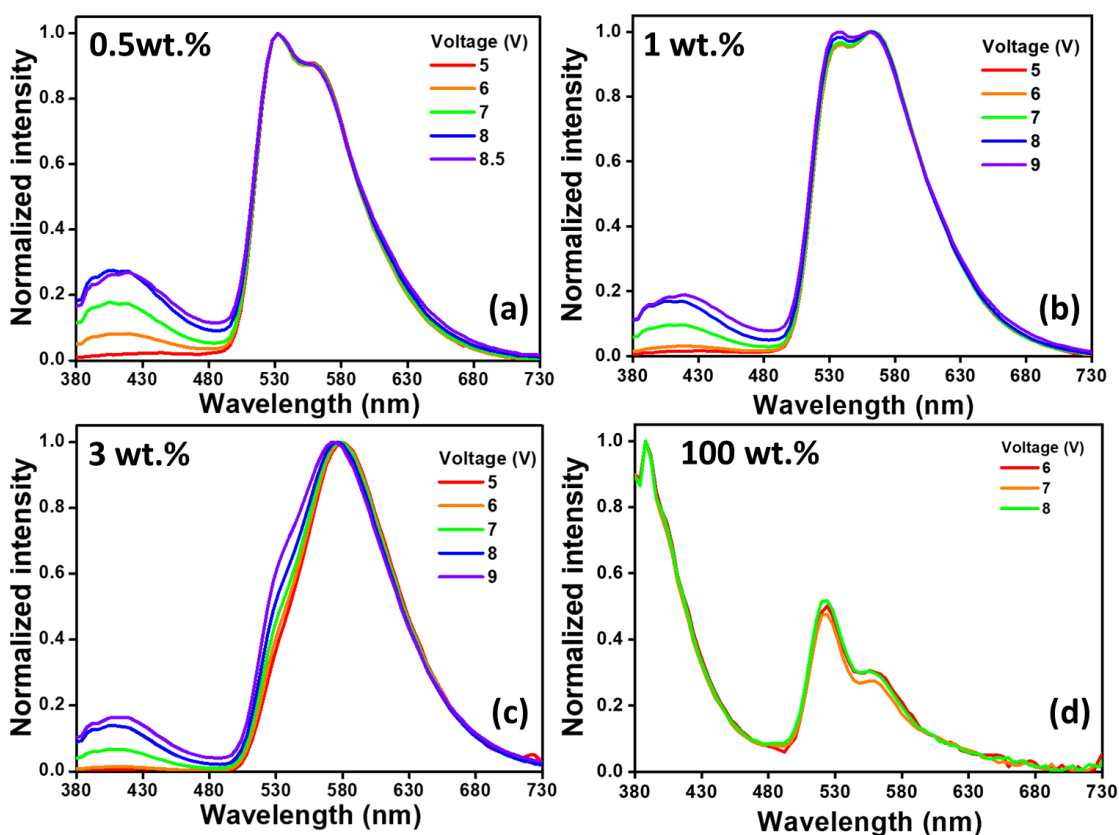


Figure S12. The electroluminescent spectra of **PEI-NST** at a varying voltage of the doped devices at varying concentrations (a) 0.5, (b) 1.0 and (c) 3.0 wt.% in the CBP host matrix, along with the (d) undoped (100 wt.%) device.

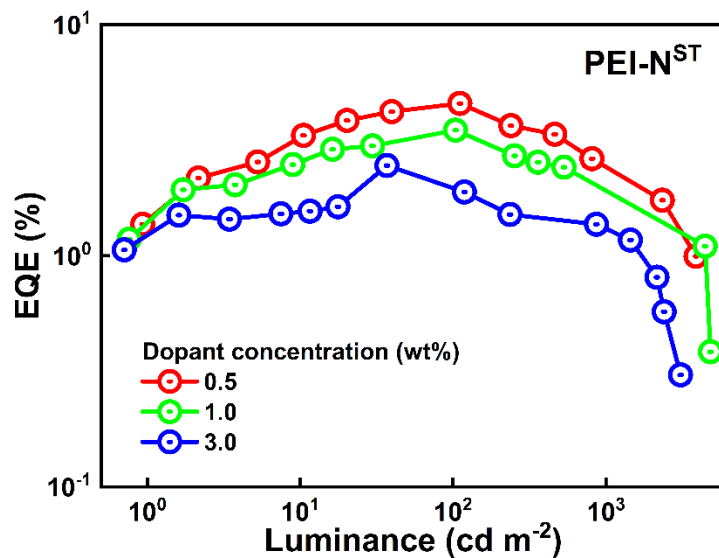


Figure S13. Electroluminescent properties of the OLED devices based on **PEI-NST** emitter doped in CBP host matrix showing EQE vs luminance characteristics.

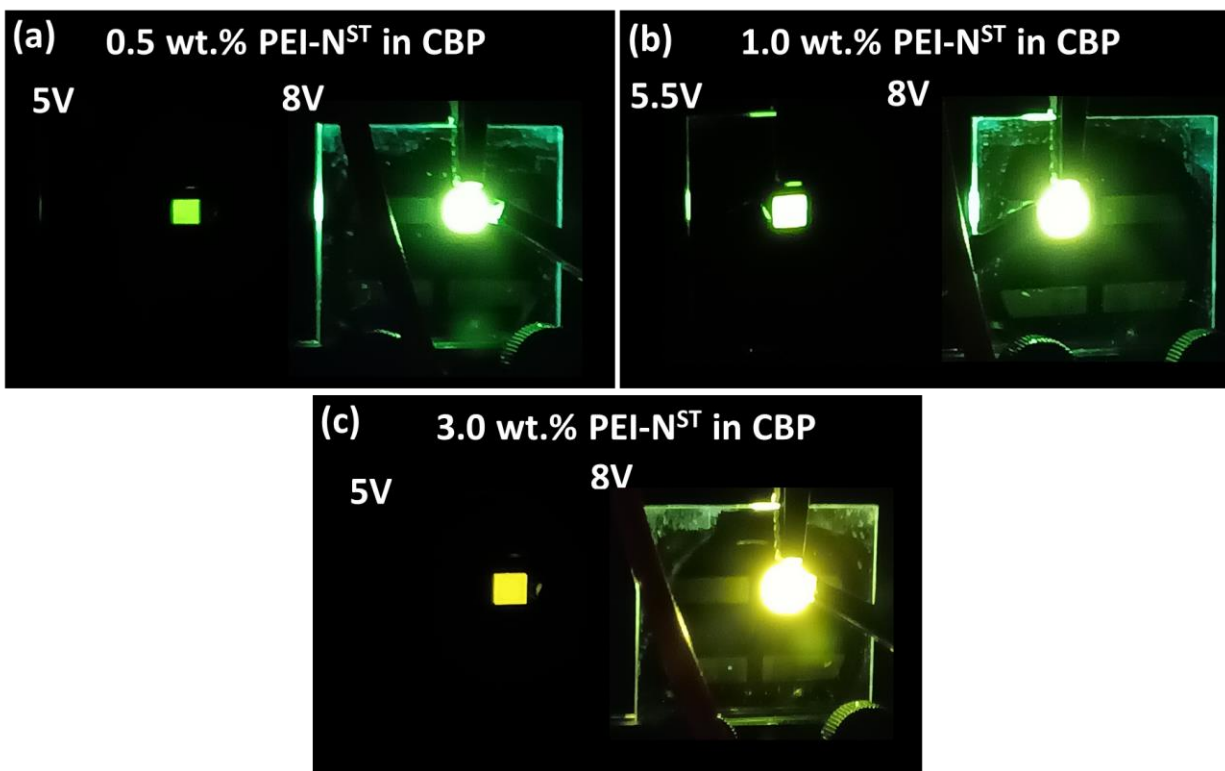


Figure S14. Emission photographs at a varying voltage for a 0.5 wt.% (a), 1.0 wt.% (b), and 3.0 wt.% (c) **PEI-NST** doped in CBP host matrix.

Table S5. A comprehensive list of the driving voltage, power efficacy, current efficacy, external quantum efficiency (EQE), CIE coordinates and luminance of the OLED device based on **PBIST** emitter doped in CBP host matrix.

PEI-N ST (wt.%)	Driving Voltage (V)	Power efficacy (lm/W)	Current efficacy (cd/A)	EQE (%)	CIE (x, y)	Maximum luminance (cd/m ²)
		@ 100/1,000 cd/m ² and max			@ 100/1,000cd/m ²	
0.5	4.2	6.6/ 3.6/ 7.0	12.6/ 8.0/ 12.6	4.3/ 2.6/4.6	(0.38, 0.56)/ (0.37, 0.53)	5,269
1.0	4.2	5.0/ 2.6/ 5.0	10.3/ 6.7/ 10.3	3.3/ 2.3/3.5	(0.42, 0.55)/ (0.41, 0.53)	4,059
3.0	4.0	2.1/ 1.4/ 3.3	4.5/ 3.4/ 4.7	2.4/ 1.3/2.5	(0.48, 0.50)/ (0.47, 0.49)	4,115
100	5.0	- / - / -	- / - / -	- / - / -	- / -	9

13. DFT Studies

To understand the electronic properties and frontier molecular orbital energy level of compounds **PEI-NST** computational studies was carried out in B3LYP/6-31g(d,p) method using Gaussian 09 program package.^{S5} The absence of imaginary frequency ensured the energy minimized structure of all the compounds.

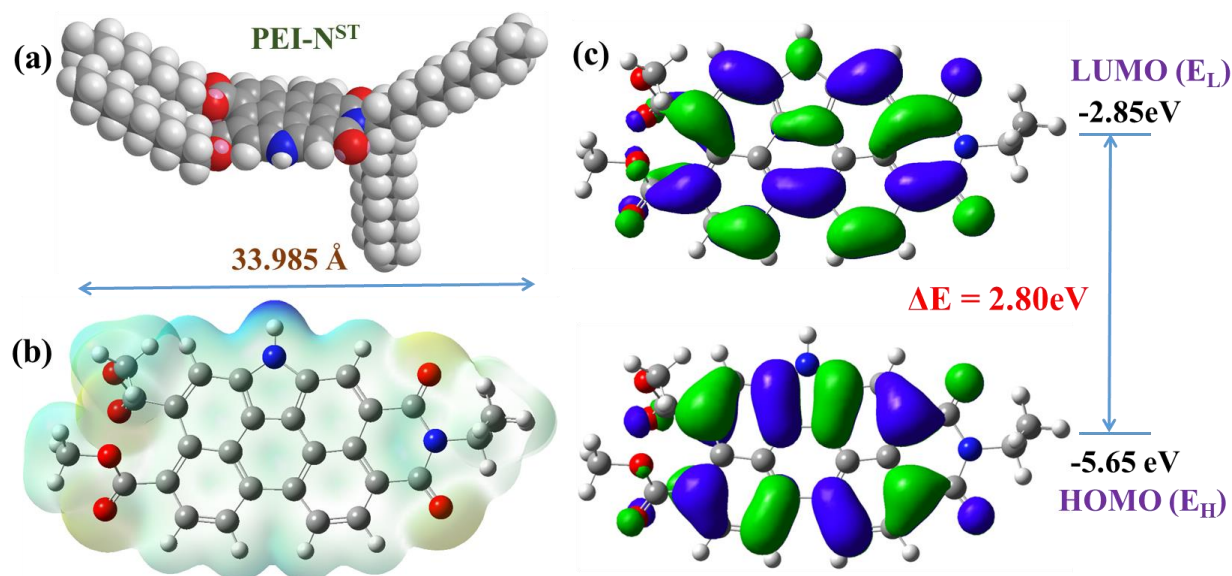


Figure S15. (a) Optimised geometry of **PEI-NST**; (b) 3D molecular electrostatic potential contour map of optimized structure of **PEI-NST** (In the mapped electro-static potential surface, the red and blue colors refer to the electron-rich and electron-poor regions, respectively, whereas the green color signifies the zero electrostatic potential, chain length is limited to methyl for clarity purpose); (c) Frontier molecular orbitals of **PEI-NST**, E_H and E_L denote energies of the highest occupied molecular orbital (HOMO) and the lowest unoccupied molecular orbital (LUMO), respectively.

DFT calculation data for PEI-NST :

Center Number	Atomic Number	Atomic Type	Coordinates (Angstroms)		
			X	Y	Z
1	6	0	-2.766696	-2.586354	0.757099
2	6	0	-1.408507	-2.719899	0.819193
3	6	0	-0.573180	-1.681895	0.505628
4	6	0	-1.252684	-0.543594	0.138762
5	6	0	-2.603987	-0.350335	0.056633
6	6	0	-3.383411	-1.423352	0.380691
7	6	0	-0.508376	0.528013	-0.179538
8	6	0	-0.920988	1.757666	-0.565193
9	6	0	-2.271467	1.930416	-0.645862
10	6	0	-3.102222	0.876613	-0.335902
11	6	0	0.827618	-1.693338	0.508034
12	6	0	1.562131	-0.570959	0.173968
13	6	0	0.830545	0.515502	-0.145380
14	6	0	1.604159	-2.767325	0.828751
15	6	0	2.948882	-2.730824	0.617180
16	6	0	3.616530	-1.627434	0.153212
17	6	0	2.931738	-0.419928	0.097402
18	6	0	3.402699	0.896167	-0.033419
19	6	0	2.590660	1.938245	-0.428854
20	6	0	1.244602	1.752367	-0.495515
21	7	0	0.170791	2.467170	-0.747823
22	6	0	-4.488503	1.039797	-0.409989
23	7	0	-5.280618	-0.066181	-0.073299
24	6	0	-4.773398	-1.313053	0.323006
25	8	0	-5.510704	-2.244137	0.601482
26	8	0	-4.998056	2.094794	-0.749304
27	6	0	-6.753959	0.090324	-0.139793
28	6	0	-7.310808	1.115440	0.872895
29	6	0	-7.256146	0.291699	-1.586560
30	6	0	-8.769653	0.095395	-1.753773
31	6	0	-6.773896	0.894921	2.294233
32	6	0	4.928042	-1.849826	-0.314837
33	8	0	5.500326	-2.913582	-0.136686
34	8	0	5.524054	-0.931275	-1.148658
35	6	0	7.932817	-1.177374	-1.172300
36	6	0	6.621982	-1.326767	-1.938227
37	6	0	4.713158	1.279980	0.298817
38	8	0	5.414898	0.559102	0.990214
39	8	0	5.150136	2.548502	0.011163
40	6	0	6.173070	3.355262	2.063975
41	6	0	6.349115	3.013715	0.587594
42	1	0	-3.359774	-3.471181	1.024891
43	1	0	-1.016818	-3.697422	1.127430
44	1	0	-2.644572	2.916026	-0.951370
45	1	0	1.165841	-3.724652	1.137161
46	1	0	3.452661	-3.698669	0.739460
47	1	0	2.950291	2.962509	-0.588564

48	1	0	0.180689	3.464405	-1.026189
49	1	0	-7.244621	-0.856307	0.170960
50	1	0	-7.096890	2.155858	0.557782
51	1	0	-8.418205	1.035277	0.908794
52	1	0	-6.993887	1.299366	-1.966562
53	1	0	-6.736439	-0.442030	-2.241561
54	1	0	-9.060124	0.176942	-2.821192
55	1	0	-9.093178	-0.904122	-1.397838
56	1	0	-9.347984	0.861816	-1.200783
57	1	0	-7.240724	1.602386	3.009622
58	1	0	-6.988118	-0.133915	2.649042
59	1	0	-5.677760	1.051576	2.345098
60	1	0	8.796252	-1.444410	-1.816020
61	1	0	8.075407	-0.132143	-0.830834
62	1	0	7.964038	-1.832839	-0.280344
63	1	0	6.478198	-2.355172	-2.325145
64	1	0	6.634581	-0.651041	-2.819600
65	1	0	7.106042	3.790664	2.477234
66	1	0	5.362495	4.099252	2.204375
67	1	0	5.926678	2.464034	2.672713
68	1	0	7.164995	2.281635	0.423133
69	1	0	6.625270	3.932398	0.028888

14. Time resolved photoluminescence studies

Fluorescence lifetime decay measurements were conducted in chloroform for **PEI-NST**. A single exponential decay with lifespan in the nanosecond time scale was detected in time resolved fluorescence studies of compound **PEI-NST**. It exhibited a lifetime of ~ 4.03 ns.

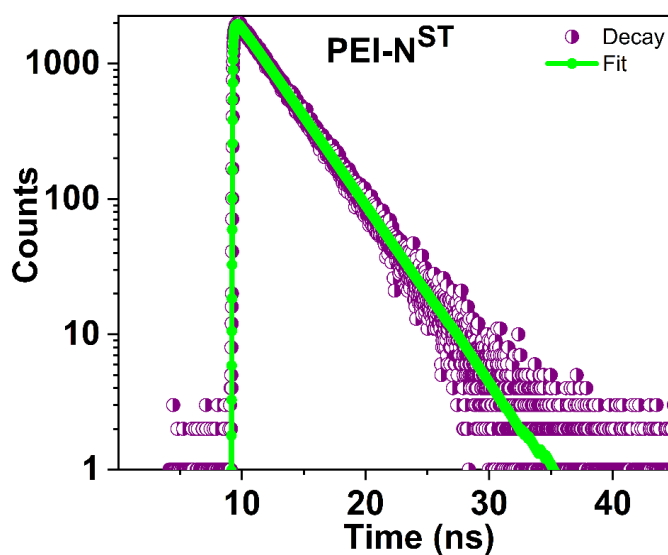


Figure S16. Fluorescence lifetime decay spectra of emitter **PEI-NST** in chloroform; Experimental decay in purple coloured circles; Mono-exponential fit in green coloured line.

15. References

- S1. R. K. Gupta, S. K. Pathak, B. Pradhan, D.S.S. Rao, S. K. Prasad, A. A. Sudhakar, *Soft Matter*, 2015, **11**, 3629-3636.
- S2. a) Gaussian 09, Revision B.01, M. J. Frisch, G. W. Trucks, H. B. Schlegel, G. E. Scuseria, M. A. Robb, J. R. Cheeseman, G. Scalmani, V. Barone, B. Mennucci, G. A. Petersson, H. Nakatsuji, M. Caricato, X. Li, H. P. Hratchian, A. F. Izmaylov, J. Bloino, G. Zheng, J. L. Sonnenberg, M. Hada, M. Ehara, K. Toyota, R. Fukuda, J. Hasegawa, M. Ishida, T. Nakajima, Y. Honda, O. Kitao, H. Nakai, T. Vreven, J. J. A. Montgomery, J. E. Peralta, F. Ogliaro, M. Bearpark, J. J. Heyd, E. Brothers, K. N. Kudin, V. N. Staroverov, R. Kobayashi, J. Normand, K. Raghavachari, A. Rendell, J. C. Burant, S. S. Iyengar, J. Tomasi, M. Cossi, N. Rega, J. M. Millam, M. Klene, J. E. Knox, J. B. Cross, V. Bakken, C. Adamo, J. Jaramillo, R. Gomperts, R. E. Stratmann, O. Yazyev, A. J. Austin, R. Cammi, C. Pomelli, J. W. Ochterski, R. L. Martin, K. Morokuma, V. G. Zakrzewski, G. A. Voth, P. Salvador, J. J. Dannenberg, S. Dapprich, A. D. Daniels, O. Farkas, J. B. Foresman, J. V. Ortiz and J. Cioslowski Fox, *D. J. Gaussian Inc., Wallingford, CT*, **2009**;
b) C. Lee, W. Yang and R. G. Parr, *Phys. Rev. B*, **1988**, 37, 785–789; c) A. D. Becke, *J. Chem. Phys.*, **1993**, 98, 1372–1377.